Contribution from the School of Chemical Sciences, University of Illinois at Urbana-Champaign, 505 South Mathews Avenue, Urbana, Illinois 61801

Structure and Photochemistry of Manganese Porphyrin Sulfate Complexes

Kenneth S. Suslick,* Randall A. Watson, and Scott R. Wilson

Received October 5, 1990

New sulfate and hydrogen sulfate complexes of metalloporphyrins have been synthesized and crystallographically characterized and their photochemistry examined. Irradiation of $[Mn(TPP)]_2(SO_4)$ and $Mn(TPP)(OSO_3H)$ (where TPP = 5,10,15,20-tetraphenylporphyrinate(2-)) produces $Mn^{II}(TPP)$ quantitatively, with quantum yields of 7.1×10^{-4} and 9.8×10^{-4}, respectively. In contrast to other manganese oxoanion complexes, metal-oxo species are not formed and oxidation of hydrocarbons does not occur. The X-ray crystal structures of $[Mn(TPP)]_2(SO_4)\cdot 2C_6H_6\cdot {}^1/_2C_5H_{12}\cdot {}^1/_2H_2O$ and $Mn(TPP)(OSO_3H)\cdot CH_2Cl_2$ show stereochemistry similar to that of the analogous iron complexes. In the sulfate complex $[Mn(TPP)]_2(SO_4)$, the average Mn-pyrrole N distance is 2.008 Å in both rings, with the metal displaced above the mean plane of the nitrogen atoms by 0.19 and 0.22 Å for Mn(1) and Mn(2), respectively. The sulfate ion is coordinated in an unidentate fashion. In $Mn(TPP)(OSO_3H)$ the average Mn-pyrrole nitrogen distance is 1.991 Å with the metal 0.23 Å above the mean plane of the nitrogen atoms. The hydrogen sulfate ion is coordinated through one of the oxygens, with Mn-O = 2.078 Å. Crystal data for $Mn(TPP)(OSO_3H)\cdot CH_2Cl_2$: space group $P\bar{1}$, a = 13.782 (8) Å, b = 13.861 (6) Å, c = 13.504 (8) Å, α = 108.57 (4)°, β = 118.77 (4)°, γ = 60.43 (4)°, V = 1956 (3) Å^3, and Z = 2. Crystal data for $[Mn(TPP)]_2(SO_4)\cdot 2C_6H_6\cdot {}^1/_2C_5H_{12}\cdot {}^1/_2H_2O$ at -25 °C: space group $P\bar{1}$, a = 14.585 (16) Å, b = 21.949 (10) Å, c = 13.142 (6) Å, α = 90.11 (4)°, β = 104.65 (6)°, γ = 96.47 (5)°, V = 4042 (9) Å^3, and Z = 2.

Introduction

Metalloporphyrins serve important biological roles in the reduction of oxoanions[1] such as nitrite and sulfite in bacteria and in the oxidation of organic substrates[2] by cytochrome P450. Only limited information is available, however, concerning the reactivity of synthetic metalloporphyrin oxoanion complexes. We report here the synthesis, characterization, and photochemistry of (μ-sulfato)bis[(5,10,15,20-tetraphenylporphyrinato)manganese(III)], $[Mn(TPP)]_2(SO_4)$, and hydrogen sulfato(5,10,15,20-tetraphenylporphyrinato)manganese(III), $Mn(TPP)(OSO_3H)$, including the single-crystal X-ray structures of both species.

We have been interested in the synthesis and reactivity of a variety of oxoanion-bound metalloporphyrins[6,7] for both their possible oxidative chemistry and their use as models of biological systems such as nitrite and sulfite reductase. Sulfite reductase carries out the six-electron reduction of SO_3^{2-} to S^{2-} in plants and bacteria.[3] The active site of sulfite reductase consists of a siroheme closely coupled to an Fe_4S_4 cluster[4] and resembles the assimilatory nitrite reductase that catalyzes the six-electron reduction of NO_2^- to NH_3.[5]

The photochemistry of both metal-free porphyrins[8] and metalloporphyrins[6-12] has generated much recent interest. Manganese metalloporphyrins have been especially examined, due to the unique mixing of metal e_g orbitals and porphyrin $e_g(\pi^*)$ orbitals.[9] The mixing of these orbitals, in so-called hyper spectra that are characterized by an intense band at low energy (470-480 nm) with additional transitions at higher energy, produce various photochemical results. For example, the photoreduction of Mn(TPP)(X) to $Mn^{II}(TPP)$, where X = I, Br, Cl, O_2CCH_3, or NCS, occurs[10a] with quantum yields of approximately 10^{-5}. The photoreduction of water-soluble manganese porphyrins has also been studied extensively.[11] In contrast to these photoreductions, manganese porphyrin perchlorates and periodates undergo photooxidation, possibly via heterolytic β-cleavage, to a putative $O{=}Mn^{IV}(TPP)^{\cdot+}$ species. This metal oxo complex is a competent oxidant of organic substrates, including alkanes. With both periodate and perchlorate complexes, all four oxygen equivalents are utilized in substrate oxidation. Manganese porphyrin nitrate and nitrite complexes also undergo photooxidation,[6] via a homolytic β-cleavage, to $O{=}Mn^{IV}(TPP)$. In the case of nitrate, two oxidizing equivalents were photogenerated, and $Mn(TPP)(NO_2)$ was shown to be a likely intermediate in the reaction. Finally, the formation of a manganese(V) nitrido complex by photooxidation of $Mn(TPP)(N_3)$ has also been reported.[12]

Experimental Section

Materials. Solvents used were of reagent grade and were distilled prior to use. Dichloromethane and chloroform were distilled from calcium hydride; toluene and heptane from sodium; pentane, diethyl ether, and benzene from sodium/benzophenone. Oxidation substrates (toluene, styrene, $P(C_6H_5)_3$) were purchased from Aldrich Chemical Co. and pu-

(1) Cole, J. A., Fergusen, S. J., Eds. *The Nitrogen and Sulphur Cycles*; Cambridge University Press: Cambridge, England 1988.

(2) Ortiz de Montellano, P. R., Ed. *Cytochrome P450*; Plenum: New York, 1985.

(3) Kemp, J. D.; Atkinson, D. E.; Ehret, A.; Lazzarini, R. A. *J. Biol. Chem.* **1961**, *238*, 3466.

(4) (a) McRee, D. E.; Richardson, D. C.; Richardson, J. S.; Siegel, L. M. *J. Biol. Chem.* **1986**, *261*, 10277. (b) Siegel, L. M.; Rueger, D. C.; Barber, M. J.; Krueger, R. J.; Orme-Johnson, W. H. *J. Biol. Chem.* **1982**, *257*, 6343. (c) Siegel, L. M.; Davis, P. S.; Kamin, H. *J. Biol. Chem.* **1974**, *249*, 1572.

(5) (a) Kuenen, J. G.; Robertson, L. A. *The Nitrogen and Sulfur Cycles*, Cole, J. A., Ferguson, S. J., Eds.; Cambridge University Press: Cambridge, England 1988; pp 161-218. (b) Lancaster, J. R.; Vega, J. M.; Kamin, H.; Orme-Johnson, N. R.; Orme-Johnson, W. H.; Krueger, R. J.; Siegel, L. M. *J. Biol. Chem.* **1979**, *254*, 1268. (c) Murphy, M. J.; Siegel, L. M.; Tore, S. R.; Kamin, H. *Proc. Natl. Acad. Sci. U.S.A.* **1974**, *71*, 612.

(6) (a) Suslick, K. S.; Watson, R. A. *Inorg. Chem.* **1991**, *30*, 912. (b) Suslick, K. S.; Bautista, J. B.; Watson, R. A. *J. Am. Chem. Soc.*, in press.

(7) (a) Suslick, K. S.; Acholla, F. V.; Cook, B. R. *J. Am. Chem. Soc.* **1987**, *109*, 2812. (b) Suslick, K. S.; Cook, B. R. In *Inclusion Phenomena and Molecular Recognition*; Atwood, J. L., Ed.; Plenum: London, 1990; pp 209-215. (c) Suslick, K. S. In *Activation and Functionalization of Alkanes*; Hill, C. L., Ed.; Wiley: New York, 1989; pp 219-241. (d) Suslick, K. S.; Cook, B. R. *J. Chem. Soc., Chem. Commun.* **1987**, 200. (e) Cook, B. R.; Reinert, T. J.; Suslick, K. S. *J. Am. Chem. Soc.* **1986**, *108*, 7281.

(8) (a) Blauer, G., Sund, H., Eds.; *Optical Properties of Tetrapyrroles*; W. DeGruyter: Berlin, 1985. (b) Gouterman, M., Rentzepis, P. M., Straub, K. D., Eds. *Porphyrins: Excited States and Dynamics*; ACS Symposium Series 321; American Chemical Society: Washington, DC, 1986. (c) Andreoni, A., Cubeddu, R., Eds. *Porphyrins in Tumor Phototherapy*; Plenum Press: New York, 1984. (d) Gomer, C. J. *Semin. Hematol.* **1989**, *26*, 27. (e) van der Bergh, H. *Chem. Brit.* **1986**, *22*, 430.

(9) Gouterman, M. In *Porphyrins*; Dolphin, D., Ed.; Academic Press: New York, 1978; Vol. 3, pp 1-166.

(10) (a) Imamura, T.; Jin, T.; Suzuki, T.; Fujimoto, M. *Chem. Lett.* **1985**, 847. (b) Hendrickson, D. N.; Kinnaird, M. G.; Suslick, K. S. *J. Am. Chem. Soc.* **1987**, *109*, 1243.

(11) (a) Carnier, N.; Harriman, A. *J. Photochem.* **1981**, *15*, 341. (b) Harriman, A.; Porter, G. *J. Chem. Soc., Faraday Trans. 2* **1980**, *76*, 1429. (c) Harriman, A.; Porter, G. *J. Chem. Soc., Faraday Trans. 2* **1979**, *75*, 1543.

(12) (a) Groves, J. T.; Takahashi, T. *J. Am. Chem. Soc.* **1983**, *105*, 2073. (b) Buchler, J. W.; Dreher, C. *Z. Naturforsch.* **1984**, *39B*, 222. (c) Jin, T.; Suzuki, T.; Imamura, T.; Fujimoto, M. *Inorg. Chem.* **1987**, *26*, 1280.

0020-1669/91/1330-2311$02.50/0

Table I. Crystallographic Data for $Mn(TPP)(OSO_3H)$ and $[Mn(TPP)]_2(SO_4)$

	(A) $Mn(TPP)(OSO_3H)\cdot CH_2Cl_2$	(B) $[Mn(TPP)]_2(SO_4)\cdot 2C_6H_6$
cryst system	triclinic	triclinic
space group	$P\bar{1}$	$P\bar{1}$
a, Å	13.782 (8)	14.585 (16)
b, Å	13.861 (6)	21.949 (10)
c, Å	13.504 (8)	13.142 (6)
α, deg	108.57 (4)	90.11 (4)
β, deg	118.77 (4)	104.65 (6)
γ, deg	60.43 (4)	97.47 (5)
V, Å^3	1956 (3)	4042 (9)
Z	2	2
T, °C	26	−25
D_{calcd}, g cm^{-3}	1.442	1.341
habit	equidimensional	platy
size of (form) or (face), mm	{001}, 0.10; {10$\bar{1}$}, 0.12; (010), 0.08; (1$\bar{1}\bar{1}$), 0.08	{100}, 0.07; {010}, 0.16; {10$\bar{3}$}, 0.26
diffractometer	Enraf-Nonius CAD4	Enraf-Nonius CAD4
λ(Mo Kα), Å	0.710 73	0.710 73
μ_{calcd}, cm^{-1}	5.61	3.83
transm coeff (numerical)	0.861–0.934	0.888–0.950
2θ limit, deg (octants)	46.0 ($\pm h,\pm k,+l$)	45.0 ($\pm h,\pm k,+l$)
intensities (unique, R_i)	5869 (5432, 0.020)	11 346 (10563, 0.019)
intensities >2.58$\sigma(I)$	2830	5579
R	0.074	0.077
R_2 (for $w = k/\sigma^2(F_o) + \rho F_o^2$)	0.086 (k = 2.4, ρ = 0.03)	0.091 (2.2, 0.03)
max density in ΔF map, e/Å^3	0.56	0.86

rified by standard procedures.[13] All substrates were passed down a short column of activity I neutral alumina immediately prior to use to remove trace contaminants and in the case of styrene to remove inhibitor. Purity was verified by gas chromatography. Inorganic salts were purchased from Aldrich and used without further purification. H_2TPP, Mn(TPP)(Cl), and $[Mn(TPP)]_2(O)$ were prepared by published methods.[14-16]

Synthesis of $Mn(TPP)(OSO_3H)$. $[Mn(TPP)]_2(O)$ (100 mg, 0.074 mmol) was dissolved in 30 mL of CH_2Cl_2. A 10% excess of 6 M H_2SO_4 (14 μL, 0.082 mmol) was then added and the mixture stirred vigorously overnight. The reaction mixture was then evaporated to dryness and the remaining solid vacuum-dried overnight. The crude solid was then dissolved in minimal CH_2Cl_2, and the mixture was filtered to remove a small amount of insoluble material, which was discarded. Addition of heptane to the CH_2Cl_2 solution results in lustrous purple needles. A second recrystallization and vacuum drying gives $Mn(TPP)(OSO_3H)$ in 85% yield. Anal. Found (calcd) for $Mn(TPP)(OSO_2H)\cdot CH_2Cl_2$: C, 63.61 (64.10); H, 3.68 (3.83); N, 6.59 (6.53); Mn, 6.46 (6.63); S, 3.77 (3.38). UV–vis in CH_2Cl_2 at 25 °C, with wavelength in nm (ϵ in L mol^{-1} cm^{-1}): 384 (3.75×10^4), 405, 470 (5.18×10^4), 521 (3.51×10^3), 574 (7.20×10^3), 608 (5.94×10^3). IR bands due to coordinated OSO_3H (KBr pellet): 1260, 1152, 1043, 874, 581 cm^{-1}.

Synthesis of $[Mn(TPP)]_2(SO_4)$. Mn(TPP)(Cl) (200 mg, 0.28 mmol) was dissolved in 50 mL of CH_2Cl_2. An equal volume of saturated Ag_2SO_4(aq) was then added and the biphasic mixture stirred vigorously for 5 h. The organic layer was filtered to remove silver salts and then dried over anhydrous Na_2SO_4. After evaporation of the solvent, the crude solid was recrystallized twice from benzene and pentane. Dark purple needles of the pure dimer were obtained in 45% yield. Anal. Found (calcd) for $[Mn(TPP)]_2(SO_4)$: C, 73.51 (73.84); H, 4.10 (3.94); N, 7.55 (7.83); Mn, 7.32 (7.68); S, 2.16 (2.24). UV–vis in CH_2Cl_2 at 25 °C, with wavelength in nm (ϵ in L mol^{-1} cm^{-1}): 374 (8.20×10^4), 397 (7.38×10^4), 466 (1.72×10^5), 528 (7.09×10^3), 575 (1.54×10^4), 612 (1.35×10^4). IR bands due to bridging SO_4 coordiantion (KBr pellet): 1385, 1108, 967, 677 cm^{-1}.

Instrumentation. UV–visible spectra were recorded on either an IBM 9430 or a Hewlett–Packard 8452A diode-array spectrophotometer. Infrared spectra were recorded as KBr pellets with either a Perkin-Elmer 1650 or 1750 FT-IR instrument. EPR were obtained with a Bruker ESP 300 ESR X-band spectrometer operating at 9.42 GHz. Temperature was maintained by a Varian ER 4111 temperature controller. Field desorption mass spectra were obtained by the SCS Mass Spectroscopy Laboratory using a Finnegan-MAT 731 instrument. Oxidation products were analyzed on a Varian 3700 GC with a Shimadzu C-R3A integrator. $P(C_6H_5)_3$ and its products were analyzed with a 0.2-mm i.d. cross-linked dimethylsilicon (HP-1) column, 12.5-m long; toluene and styrene were anlyzed with a similar column 30-m long. Dodecane was used as the internal standard for calculating yields. Product identification was confirmed by GC-mass spectral analysis. Elemental analyses were performed by the UIUC Elemental Analysis Facility.

Photochemical Reactions. All photochemical reaction solutions were prepared in a Vacuum-Atmospheres inert-atmosphere box (<2 ppm O_2) and sealed in cuvettes to avoid complications that might otherwise be caused by the presence of oxygen. Reaction solutions were generally 300 mM in substrate and 0.3 mM in porphyrin. All reactions were run in benzene. An aliquot of dodecane was included in each mixture as an internal standard for GC analysis. Irradiation was carried out with a 300-W xenon arc lamp focused onto the reaction cuvette. Wavelengths were selected by the use of various band-pass filters. Cuvettes were thermostated. Quantum yields were determined by chemcial actinometry with Aberchrome 540,[17] at 366 nm, using a 450-W medium-pressure Hg-arc immersion lamp.

Structure Determination and Refinement of $Mn(TPP)(OSO_3H)\cdot CH_2Cl_2$. Crystals suitable for X-ray analysis were obtained by the slow diffusion of pentane into a methylene chloride solution of the porphyrin. Crystal and experimental data are given in Table IA. The crystal was mounted with epoxy to a thin glass fiber, and data were collected at 26 °C. There was no change in the appearance of the sample during the experiment. The data were corrected for a 23% decay as a linear function of exposure time and were corrected for absorption, anomalous dispersion, Lorentz, and polarization effects.

The structure was solved by Patterson methods (SHELXS-86);[18] the correct manganese position was deduced from a Patterson map. A weighted difference Fourier synthesis revealed positions for the atoms of the porphyrin ring and the sulfate group. Subsequent least-squares difference Fourier calculations gave positions for the remaining non-hydrogen atoms. Hydrogen atoms were included as fixed contributors in "idealized" positions. In the final cycle of least squares, isotropic thermal coefficients were refined for the phenyl atoms and anisotropic thermal coefficients for the remaining non-hydrogen atoms, and a group isotropic thermal parameter was varied for the hydrogen atoms. Successful convergence was indicated by the maximum shift/error for the last cycle. Thermal parameters for the solvent molecules were extremely large, but attempts to describe a disorder model were unsuccessful. The thermal parameters for carbon atoms C29–31 and C41–43 were larger than the mean for aromatic carbon atoms in this structure. Covalent bond lengths between these carbon atoms were significantly shorter than expected. The highest peaks in the final difference Fourier map were located in the vicinity of carbon atoms C29–31 and C41–43, but there were no other

(13) Perrin, D. D.; Armarego, W. L. F. *Purification of Laboratory Chemicals*, 3rd ed.; Pergammon: Oxford, England, 1988.
(14) Adler, A. D.; Longo, F. R.; Finarelli, J. D. *J. Org. Chem.* **1967**, *32*, 476.
(15) (a) Boucher, L. J. *J. Am. Chem. Soc.* **1968**, *90*, 6640. (b) Boucher, L. J. *Coord. Chem. Rev.* **1972**, *7*, 289.
(16) Fleischer, E. B. *J. Am. Chem. Soc.* **1971**, *93*, 3162.
(17) (a) Heller, H. G.; Langan, J. R. *J. Chem. Soc., Perkin Trans. 2* **1981**, 341. (b) Darcy, P. J.; Heller, H. G.; Strydom, P. J.; Whittall, J. *J. Chem. Soc., Perkin Trans. 2* **1981**, 202.
(18) Sheldrick, G. M. In *Crystallographic Computing B*; Sheldrick, G. M.; Kruger, G.; Goddard, R., Eds.; Oxford University Press: Oxford England, 1985; pp 175–189.

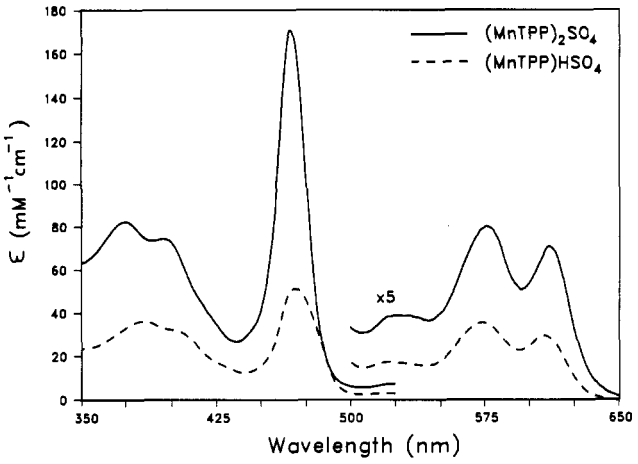

Figure 1. Electronic spectra in CH_2Cl_2: (—) $[Mn(TPP)]_2(SO_4)$ (λ_{max} = 374, 397, 466, 528, 575, 612 nm); (---) $Mn(TPP)(OSO_3H)$ (λ_{max} = 384, 405, 470, 521, 574, 608 nm).

significant features in the map. There was no obvious disorder model to account for these abnormalities. Crystal decomposition, probably involving loss of the solvate molecule, may be responsible for distortions in the proposed structural model. A final analysis of variance between observed and calculated structure factors showed no apparent systematic errors.

Structural Determination and Refinement of $[Mn(TPP)]_2(SO_4)\cdot 2C_6H_6\cdot{}^1/_2C_5H_{12}\cdot{}^1/_2H_2O$. Crystals suitable for X-ray analysis were obtained by slow diffusion of pentane into a benzene solution. Crystal and experimental data are given in Table IB. The crystal was mounted with epoxy, and data were collected at −25 °C. There was no change in the appearance of the sample during the experiment. Typical ω-scan widths exceeded 0.4° at half-maximum. The data were corrected for absorption, anomolous dispersion, Lorentz, and polarization effects.

The structure was solved by direct methods (SHELXS-86);[18] correct positions for the manganese and sulfur atoms were deduced from an *E* map. Subsequent least-squares difference Fourier calculations revealed positions for the remaining non-hydrogen atoms, including two disordered benzene solvate molecules, a pentane solvate disordered about an inversion center, and a partially occupied water site.[19] Hydrogen atoms on the porphyrin molecule were included as fixed contributors in idealized positions. Hydrogen atoms on disordered carbon atoms were not included in strucure factor calculations. Phenyl group orientations were refined with "ideal" ring geometry. In the final cycles of block-matrix least-squares refinement, common isotropic thermal parameters were varied for hydrogen and disordered non-hydrogen atoms, isotropic thermal coefficients were refined for phenyl and solvent non-hydrogen atoms, and anisotropic thermal coefficients were refined for the remaining non-hydrogen atoms. Successful convergence was indicated by the maximum shift/error for the final cycles. The highest peaks in the final difference Fourier map were in the vicinity of the disordered sulfate group. A final analysis of variance between observed and calculated structure factors showed a slight inverse dependence on sine θ.

Results and Discussion

Synthesis and Characterization. We have successfully synthesized both $[Mn(TPP)]_2(SO_4)$ and $Mn(TPP)(OSO_3H)$ and have solved both crystal structures. $[Mn(TPP)]_2(SO_4)$ was prepared by the reaction of Mn(TPP)(Cl) with Ag_2SO_4(aq) in a biphasic methylene chloride/water system. The formation of insoluble AgCl drives the reaction by removing Cl^- as a competing ligand. The product was identified by field desorption mass spectroscopy (FD-MS), which gives a parent ion cluster centered around 1431 amu. The monodentate bridging coordination of the sulfate anion was confirmed by the positions and number of new absorbances in the infrared spectrum (Figure 2).[20] Not surprisingly, the

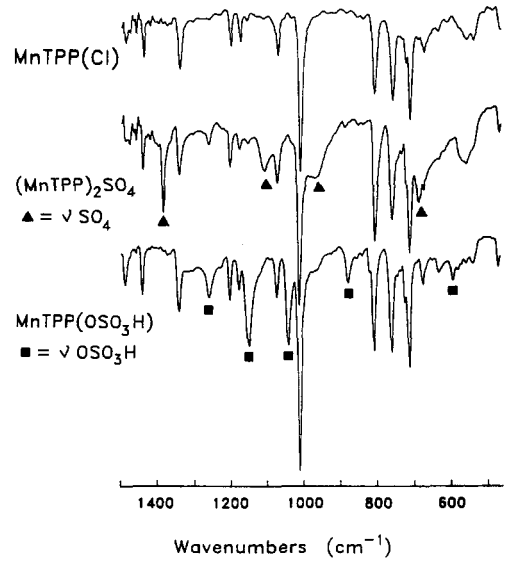

Figure 2. Infrared spectra of manganese porphyrin complexes (KBr pellet): Mn(TPP)(Cl); $[Mn(TPP)]_2(SO_4)$, $\nu(SO_4)$ = 1385, 1108, 967, 677 cm^{-1}; $Mn(TPP)(OSO_3H)$, $\nu(OSO_3H)$ = 1260, 1152, 1043, 874, 581 cm^{-1}.

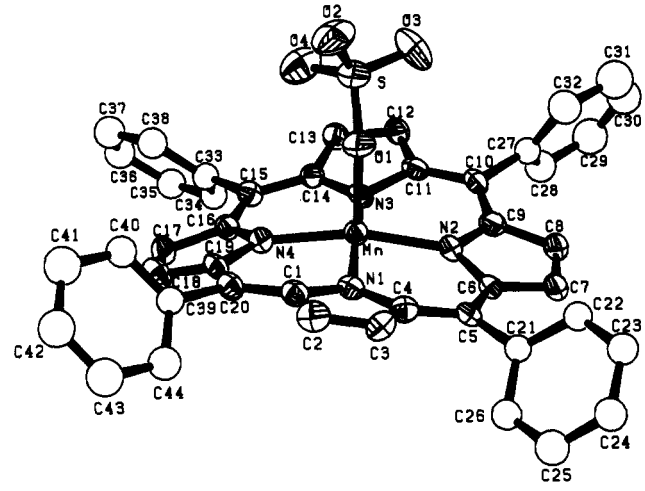

Figure 3. ORTEP diagram of $Mn(TPP)(OSO_3H)$, showing atom-labeling scheme used in all tables.

UV–visible spectrum shows no unusual features, indicative of only weak interaction between the two porphyrin moieties.

The synthesis of $Mn(TPP)(OSO_3H)$ was accomplished by acid cleavage of $[Mn(TPP)]_2(O)$ in methylene chloride with H_2SO_4. As shown in Figure 1, the electronic spectrum of the monomer is essentially identical with that of the dimer (but with roughly half the extinction coefficient, as expected), suggesting similar manganese coordination. The infrared spectrum (Figure 2) is consistent with a monodentate hydrogen sulfate complex and is supported by FD-MS (parent peak at 764 amu). Neither the mass spectrum nor the infrared spectrum show any contamination with the sulfate dimer. Subsequent tests showed no propensity for the hydrogen sulfate monomer to dimerize to the μ-sulfato form in organic solvents. This is in contrast to the iron system, which on redissolution gives exclusively $[Fe(TPP)]_2(SO_4)$ as product.[20] It is also interesting to note that the synthesis of $Mn(TPP)(OSO_3H)$ by acid cleavage of the μ-oxo dimer has been used in the case of Fe(TPP) to form the μ-sulfato dimer.[21-23]

(19) Benzene solvate molecules were constrained to ideal ring geometry. Relative group "A" site occupancy for C89–94 converged at 0.566 (4) and for C95–00 at 0.398 (5). The geometry of the inversion disordered pentane was grossly distorted but nevertheless serves to identify the approximate positions of this solvate. The oxygen atom site representing a water solvate converged with a partial occupancy of 0.50 (1). This site, O1x, cannot be occupied coincident with site O2B but is within 2.8 Å of atom O2A, suggesting a possible hydrogen bond.

(20) Nakamoto, K. *Infrared and Raman Spectra of Inorganic and Coordination Compounds*, 3rd ed.; Wiley: New York, 1978; pp 239–242.
(21) Scheidt, W. R.; Lee, Y. J.; Finnegan, M. G. *Inorg. Chem.* **1988**, *27*, 4725.
(22) Phillippi, M. A.; Baenziger, N.; Goff, H. M. *Inorg. Chem.* **1981**, *20*, 3904.

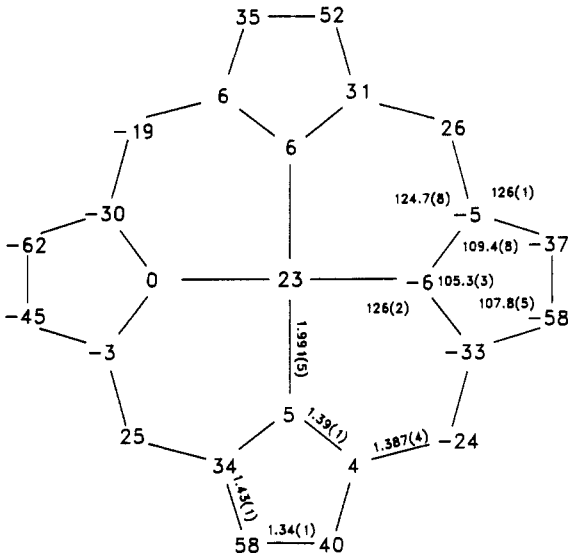

Figure 4. Formal diagram of the porphyrinato core of Mn(TPP)(OSO_3H) with average bond distances and angles in the core and displacement of atoms from the mean 24-atom plane (in 0.01-Å units).

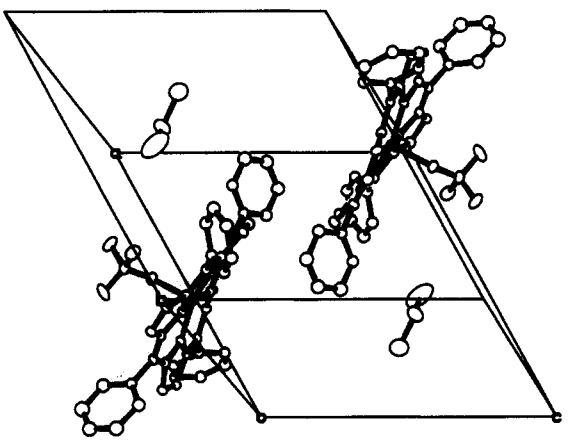

Figure 5. Unit cell packing arrangement of Mn(TPP)(OSO_3H), showing placement of CH_2Cl_2 solvate molecules.

Crystal Structures. Refinement of the structure of Mn(TPP)(OSO_3H) confirms the monodentate coordination mode already suggested by the IR spectrum. The molecular strucure is given in Figure 3 along with the atom-labeling scheme. Atomic coordinates for all porphyrinic atoms are given in Table II. Table III contains values for selected bond distances and angles. Figure 4 gives the displacement of each atom from the 24-atom core showing an S_4 ruffling. Figure 5 shows the unit cell packing arrangement. The average Mn–N_{por} distance of 1.991 (6) Å and the Mn–core displacement are within the range observed for other manganese(III) porphyrin complexes. The Mn–O bond distance of 2.078 (5) Å is similar to the Mn–O distance observed in the nitrate (2.101 (3) Å) and nitrite complexes[6] (2.059 (4) Å) and is longer than the Fe–O distance of 1.926 Å in Fe(TPP)(OSO_3H).[21]

While the hydrogen atom of the bisulfate ligand was not located, examination of the sulfur–oxygen bond lengths suggest that it may be disordered between oxygen atoms O2 and O4. A preference for O2 is suspected on the basis of the strong potential for hydrogen bonding across the inversion center. This model is in agreement with that proposed[21] for Fe(TPP)(OSO_3H). As such, the largest S–O distance involves the oxygen that is most likely to be bonded to the hydrogen; next comes the oxygen that is the hydrogen-bond acceptor, followed very closely by the metal-bound oxygen; the shortest S–O distance involves the noncoordinated terminal oxygen.

(23) Scheidt, W. R.; Lee, Y. J.; Bartzcak, T.; Hatano, K. *Inorg. Chem.* **1984**, *23*, 2552.

Table II. Atomic Coordinates for Mn(TPP)(OSO_3H)

atom	x/a	y/b	z/c
Mn	0.2392 (1)	0.4613 (1)	0.0386 (1)
S	0.3447 (3)	0.4841 (3)	−0.1238 (3)
O1	0.3340 (6)	0.4249 (5)	−0.0597 (5)
O2	0.4654 (8)	0.4125 (7)	−0.1360 (7)
O3	0.2496 (9)	0.5009 (9)	−0.2333 (7)
O4	0.3513 (7)	0.5903 (7)	−0.0561 (8)
N1	0.3367 (7)	0.3111 (6)	0.0949 (6)
N2	0.1136 (7)	0.4072 (7)	−0.0796 (6)
N3	0.1271 (6)	0.6163 (6)	0.0003 (6)
N4	0.3421 (7)	0.5221 (7)	0.1826 (6)
C1	0.4556 (8)	0.2749 (8)	0.1732 (8)
C2	0.5104 (9)	0.1559 (8)	0.1628 (9)
C3	0.4262 (9)	0.1201 (8)	0.0824 (9)
C4	0.3168 (9)	0.2151 (8)	0.0405 (8)
C5	0.2087 (9)	0.2113 (8)	−0.0423 (7)
C6	0.1108 (9)	0.3030 (8)	−0.0971 (7)
C7	−0.0033 (9)	0.3052 (9)	−0.1871 (8)
C8	−0.0651 (9)	0.4048 (9)	−0.2295 (8)
C9	0.0072 (9)	0.4677 (9)	−0.1628 (8)
C10	−0.0258 (8)	0.5746 (9)	−0.1824 (7)
C11	0.0304 (9)	0.6433 (9)	−0.1061 (8)
C12	−0.0050 (8)	0.7555 (9)	−0.1175 (8)
C13	0.0629 (9)	0.7988 (8)	−0.0206 (8)
C14	0.1440 (8)	0.7139 (8)	0.0532 (8)
C15	0.2298 (8)	0.7232 (8)	0.1624 (8)
C16	0.3174 (8)	0.6328 (8)	0.2248 (8)
C17	0.4038 (9)	0.6378 (9)	0.3384 (8)
C18	0.4823 (9)	0.5342 (9)	0.3632 (8)
C19	0.4485 (8)	0.4609 (8)	0.2673 (8)
C20	0.5071 (8)	0.3448 (8)	0.2580 (8)
C21	0.2012 (8)	0.1015 (8)	−0.0775 (8)
C22	0.1733 (8)	0.0533 (8)	−0.1913 (8)
C23	0.1756 (9)	−0.0529 (8)	−0.2203 (9)
C24	0.2013 (9)	−0.1108 (9)	−0.1406 (9)
C25	0.2286 (9)	−0.0664 (9)	−0.0293 (9)
C26	0.2279 (8)	0.0393 (8)	0.0026 (8)
C27	−0.1306 (8)	0.6178 (8)	−0.2894 (8)
C28	−0.2414 (10)	0.6998 (9)	−0.2929 (10)
C29	−0.338 (1)	0.733 (1)	−0.400 (1)
C30	−0.318 (1)	0.682 (1)	−0.494 (1)
C31	−0.216 (1)	0.604 (1)	−0.495 (1)
C32	−0.117 (1)	0.5691 (10)	−0.3905 (10)
C33	0.2289 (9)	0.8359 (8)	0.2155 (8)
C34	0.1291 (9)	0.9223 (8)	0.2331 (8)
C35	0.1332 (10)	1.0235 (9)	0.2902 (9)
C36	0.2383 (10)	1.0380 (9)	0.3315 (9)
C37	0.339 (1)	0.9527 (9)	0.3143 (9)
C38	0.3357 (10)	0.8507 (9)	0.2553 (9)
C39	0.6337 (8)	0.2962 (8)	0.3459 (8)
C40	0.7193 (9)	0.3293 (8)	0.3615 (8)
C41	0.837 (1)	0.2847 (10)	0.4468 (10)
C42	0.862 (1)	0.2100 (10)	0.509 (1)
C43	0.780 (1)	0.175 (1)	0.4945 (10)
C44	0.6614 (10)	0.2183 (9)	0.4098 (9)

Table III. Selected Bond Lengths (Å) and Angles (deg) in Mn(TPP)(OSO_3H)

Bond Lengths			
Mn–N1	1.994 (7)	S–O1	1.462 (4)
Mn–N2	1.991 (8)	S–O2	1.520 (9)
Mn–N3	1.983 (7)	S–O3	1.418 (10)
Mn–N4	1.996 (8)	S–O4	1.486 (9)
Mn–O1	2.078 (5)		
Bond Angles			
N1–Mn–O1	93.6 (3)	O1–S–O3	112.0 (5)
N2–Mn–O1	96.8 (2)	O1–S–O4	109.2 (5)
N3–Mn–O1	96.7 (2)	O2–S–O3	109.2 (5)
N4–Mn–O1	98.5 (2)	O2–S–O4	106.9 (4)
Mn–O1–S	138.2 (4)	O3–S–O4	112.4 (6)
O1–S–O2	106.9 (4)		

The only significant difference between the structures of Mn(TPP)(OSO_3H) and Fe(TPP)(OSO_3H) is that the S–O distance of the iron-bound oxygen is slightly longer than that of the hydrogen-bond-acceptor oxygen in the iron complex.

Table IV. Atomic Coordinates for $[Mn(TPP)]_2(SO_4)$

	x/a	y/b	z/c
Mn1	-0.10809 (9)	0.59654 (6)	-0.0054 (1)
Mn2	0.04516 (9)	0.87787 (6)	0.0284 (1)
S(A)	0.0004 (2)	0.7325 (1)	0.0348 (3)
S(B)	-0.0358 (7)	0.7389 (3)	0.0640 (5)
O1A	0.0796 (6)	0.7206 (4)	-0.0034 (7)
O2A	0.0170 (7)	0.7298 (4)	0.1485 (6)
O1B	-0.093 (1)	0.7515 (9)	0.133 (1)
O2B	0.059 (1)	0.7238 (9)	0.115 (2)
O3	-0.0857 (3)	0.6886 (2)	-0.0147 (4)
O4	-0.0275 (4)	0.7937 (2)	-0.0020 (5)
N1	-0.0796 (5)	0.5792 (3)	-0.1431 (6)
N2	0.0261 (5)	0.5825 (3)	0.0686 (5)
N3	-0.1414 (5)	0.5958 (3)	0.1338 (6)
N4	-0.2486 (5)	0.5832 (3)	-0.0769 (5)
N5	0.0267 (5)	0.9010 (3)	-0.1227 (6)
N6	0.1789 (5)	0.8611 (3)	0.0324 (6)
N7	0.0763 (5)	0.8740 (3)	0.1859 (5)
N8	-0.0697 (5)	0.9191 (3)	0.0321 (5)
C1	-0.1430 (6)	0.5766 (4)	-0.2424 (7)
C2	-0.0912 (7)	0.5816 (4)	-0.3221 (8)
C3	0.0011 (6)	0.5856 (4)	-0.2722 (7)
C4	0.0094 (6)	0.5849 (4)	-0.1606 (7)
C5	0.0961 (6)	0.5873 (4)	-0.0840 (7)
C6	0.0998 (6)	0.5832 (4)	0.0216 (7)
C7	0.1880 (6)	0.5824 (4)	0.1014 (8)
C8	0.1668 (6)	0.5843 (4)	0.1949 (8)
C9	0.0659 (6)	0.5860 (4)	0.1758 (7)
C10	0.0206 (6)	0.5947 (4)	0.2538 (7)
C11	-0.0775 (6)	0.5984 (4)	0.2320 (7)
C12	-0.1278 (7)	0.6069 (5)	0.3116 (8)
C13	-0.2193 (7)	0.6094 (5)	0.2619 (8)
C14	-0.2288 (7)	0.6043 (4)	0.1513 (7)
C15	-0.3130 (6)	0.6033 (4)	0.0751 (7)
C16	-0.3218 (6)	0.5905 (4)	-0.0309 (8)
C17	-0.4102 (6)	0.5853 (4)	-0.1117 (8)
C18	-0.3910 (6)	0.5733 (4)	-0.2040 (8)
C19	-0.2905 (6)	0.5745 (4)	-0.1845 (7)
C20	-0.2408 (6)	0.5711 (4)	-0.2618 (7)
C21	-0.0581 (6)	0.9153 (4)	-0.1897 (7)
C22	-0.0517 (7)	0.9117 (4)	-0.2957 (7)
C23	0.0353 (6)	0.8959 (4)	-0.2946 (7)
C24	0.0846 (6)	0.8890 (4)	-0.1885 (7)
C25	0.1738 (6)	0.8719 (4)	-0.1561 (7)
C26	0.2176 (6)	0.8587 (4)	-0.0528 (8)
C27	0.3101 (6)	0.8396 (5)	-0.0179 (8)
C28	0.3242 (7)	0.8263 (5)	0.0843 (8)
C29	0.2430 (6)	0.8399 (4)	0.1169 (8)
C30	0.2304 (6)	0.8334 (4)	0.2177 (7)
C31	0.1516 (6)	0.8474 (4)	0.2481 (7)
C32	0.1387 (7)	0.8409 (4)	0.3529 (7)
C33	0.0568 (7)	0.8615 (4)	0.3523 (8)
C34	0.0153 (6)	0.8824 (4)	0.2486 (7)
C35	-0.0677 (6)	0.9080 (4)	0.2196 (7)
C36	-0.1039 (6)	0.9292 (4)	0.1190 (7)
C37	-0.1888 (7)	0.9585 (4)	0.0879 (8)
C38	-0.2070 (6)	0.9649 (4)	-0.0159 (7)
C39	-0.1356 (6)	0.9398 (4)	-0.0521 (7)
C40	-0.1321 (6)	0.9342 (4)	-0.1561 (7)
C41	0.1866 (4)	0.6003 (2)	-0.1149 (4)
C47	0.0757 (4)	0.6097 (3)	0.3635 (5)
C53	-0.3979 (4)	0.6173 (2)	0.1091 (5)
C59	-0.2990 (5)	0.5654 (3)	-0.3738 (5)
C65	0.2292 (4)	0.8645 (2)	-0.2357 (4)
C71	0.3069 (4)	0.8053 (2)	0.2961 (5)
C77	-0.1261 (4)	0.9133 (3)	0.2962 (5)
C83	-0.2201 (4)	0.9462 (2)	-0.2378 (4)

The refined structure of $[Mn(TPP)]_2(SO_4)$ reveals a bridging monodentate sulfate coordination (Figure 6). Atomic coordinates of porphyrinic atoms excluding phenyl rings are listed in Table IV. Table V contains values for selected bond distances and angles. Each of the independent porphyrin rings of the dimer are shown in Figure 7 with the displacement of each atom from the 24-atom core. Both exhibit S_4 ruffling although not as pronounced as in $Mn(TPP)(OSO_3H)$. Figure 8 shows the unit cell packing arrangement. The average $Mn-N_{por}$ distance of 2.008 (5) Å in both rings and the Mn–core displacement of 0.19 and 0.22 Å for Mn(1) and Mn(2), respectively, are within the range observed for other manganese(III) porphyrins.

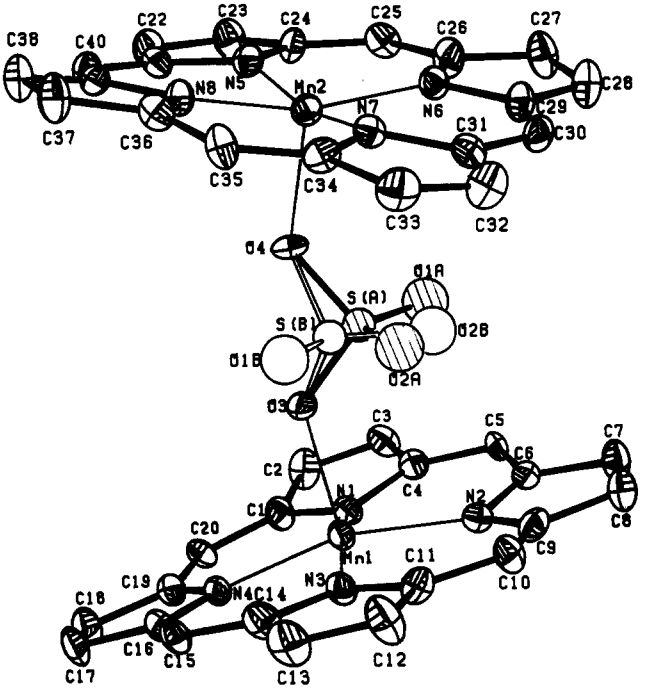

Figure 6. ORTEP diagram of $[Mn(TPP)]_2(SO_4)$ porphyrin core, showing the atom-labeling scheme used in all tables and the disorder of the sulfate group. The phenyl rings have been removed for clarity.

Table V. Selected Bond Lengths (Å) and Angles (deg) in $[Mn(TPP)]_2(SO_4)$

Bond Lengths			
Mn1-N1	2.002 (7)	S(A)-O2A	1.455 (9)
Mn1-N2	2.011 (7)	S(A)-O4	1.493 (5)
Mn1-N3	2.007 (7)	Mn2-O4	2.008 (5)
Mn1-N4	2.014 (7)	Mn2-N5	2.010 (7)
Mn1-O3	2.019 (5)	Mn2-N6	2.013 (7)
S(A)-O3	1.498 (6)	Mn2-N7	2.008 (7)
S(A)-O1A	1.419 (9)	Mn2-N8	2.002 (7)
Bond Angles			
N1-Mn1-O3	94.6 (2)	O2A-S(A)-O3	108.2 (5)
N2-Mn1-O3	97.9 (2)	O2A-S(A)-O4	110.5 (5)
N3-Mn1-O3	96.8 (2)	O3-S(A)-O4	104.1 (3)
N4-Mn1-O3	99.2 (2)	Mn2-O4-S(A)	130.6 (4)
Mn1-O3-S(A)	129.9 (3)	N5-Mn2-O4	96.0 (3)
O1A-S(A)-O2A	114.2 (6)	N6-Mn2-O4	101.9 (3)
O1A-S(A)-O3	110.7 (5)	N7-Mn2-O4	96.6 (3)
O1A-S(A)-O4	108.6 (5)	N8-Mn2-O4	94.4 (3)

The stereochemistry of the sulfate is similar to that in the iron complex.[23] The Mn1–O3 and Mn2–O4 distances of 2.019 (5) and 2.008 (5) Å are on the short end of the range observed for other O-bound ligands. As with other O-bound ligands, the Mn–O bond lengths are slightly longer than the Fe–O bond length in analogous complexes. One reason for this general observation may be the smaller metal out-of-plane displacement of manganese. The sulfur and terminal oxygen atoms were disordered in two positions with relative site occupancy 0.791 (3) for group "A". Nevertheless, sulfate bond distances and angles are similar to those in the iron system and are typical of coordinated sulfate. The dihedral angle between the porphyrin cores is 22° (compared to 24° in the iron). The Mn1–Mn2 separation of 6.30 Å is longer than the 6.05 Å observed in the iron case, reflecting longer M–O bond distances. There are no significant interactions between the porphyrin cores.

Photochemistry. On irradiation between 350 and 420 nm, both $[Mn(TPP)]_2(SO_4)$ and $Mn(TPP)(OSO_3H)$ cleanly produce $Mn^{III}(TPP)$ in >90% yield. In the case of $Mn(TPP)(OSO_3H)$ this process occurs with a quantum yield of 9.8×10^{-4} with isosbestic

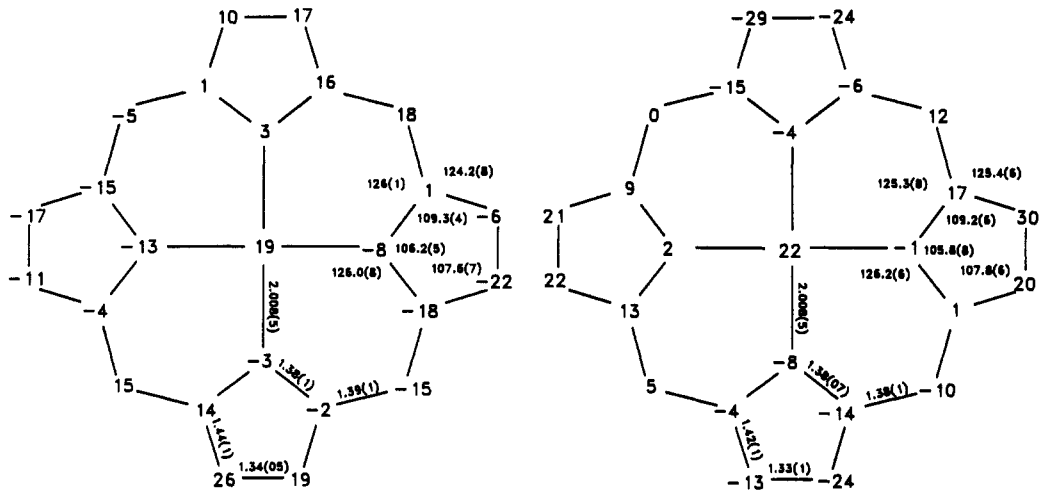

Figure 7. Formal diagram of the porphyrinato cores of $[Mn(TPP)]_2(SO_4)$ with average bond distances and angles in the cores and displacement of atoms from the mean 24-atom planes (in 0.01-Å units).

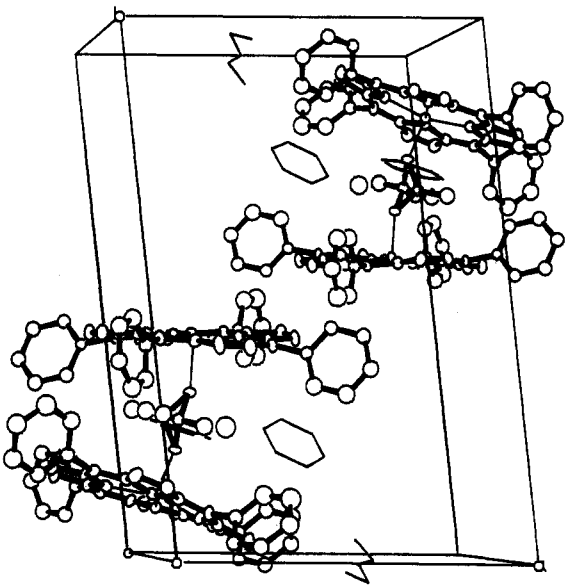

Figure 8. Unit cell packing arrangement of $[Mn(TPP)]_2(SO_4)$, showing disordered SO_4 positions and the partially occupied solvate water molecule site.

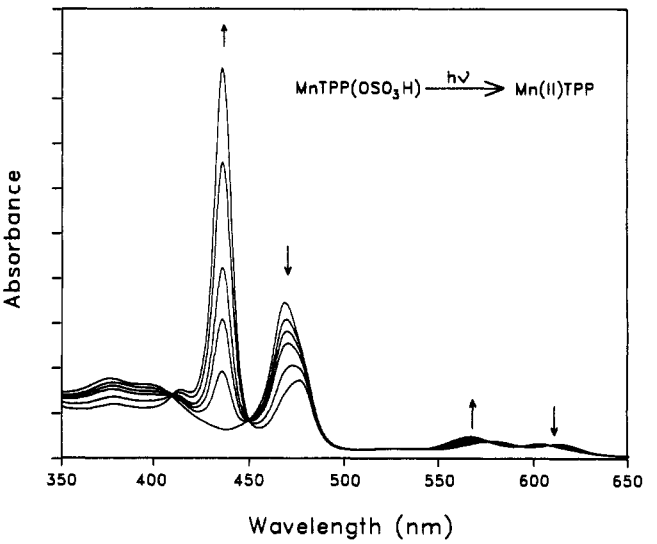

Figure 9. Photolytic conversion of $Mn(TPP)(OSO_3H)$ to $Mn^{II}(TPP)$ in benzene on irradiation from 350 to 440 nm. Arrows indicate the change in absorbance during irradiation. Isosbestic points occur at 409, 450, 537, 576, 594, and 608 nm.

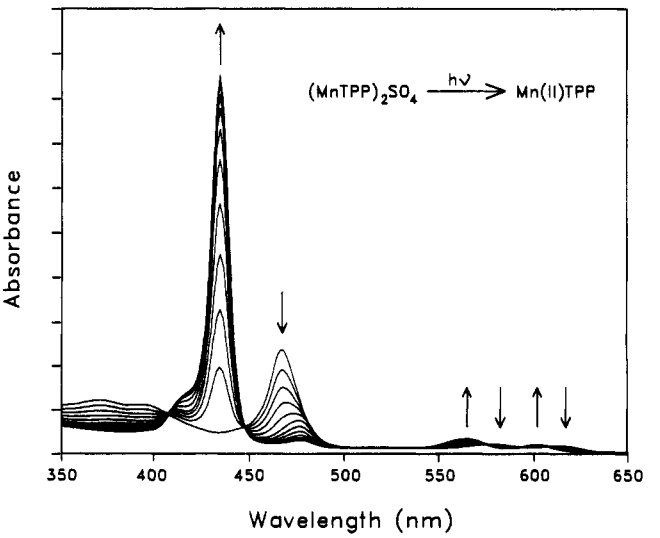

Figure 10. Photolytic conversion of $[Mn(TPP)]_2(SO_4)$ to $Mn^{II}(TPP)$ in benzene on irradiation from 350 to 440 nm. Arrows indicate the change in absorbance during irradiation. Isosbestic points occur at 407, 448, 539, 572, 594, and 609 nm.

points at 409, 450, 537, 576, 594, and 608 nm (Figure 9). Similarly, photolysis of $[Mn(TPP)]_2(SO_4)$ has a quantum yield of $Mn^{II}(TPP)$ production of 7.1×10^{-4} and isosbestic points at 407, 448, 539, 572, 594, and 609 nm (Figure 10). In both cases, $Mn^{II}(TPP)$ was identified from its electronic and EPR spectra.[24]

In our earlier studies with manganese porphyrin nitrates,[6] perchlorates, and periodates,[7] metal–oxo species were formed on photolysis ($O{=}Mn^{IV}(TPP)$ in the nitrate systems, $O{=}Mn^{IV}(TPP)^+$ in the perchlorate and periodate systems). No evidence for similar species, however, was obtained with $[Mn(TPP)]_2(SO_4)$ or $Mn(TPP)(OSO_3H)$. The formation of $O{=}Mn^{IV}(TPP)$ may be ruled out on spectroscopic evidence. The $O{=}Mn^{IV}(TPP)$ species are known to be stable enough at room temperature to make direct observation possible.[6,25] The formation of $O{=}Mn^{IV}(TPP)^+$, which reacts too quickly at room temperature to be observed easily,[25] cannot be ruled out on spectroscopic data alone. If $O{=}Mn^{IV}(TPP)^+$ were formed, however, both epoxidation and hydroxylation of substrates should be observed.[7,25] In several reactions using styrene or toluene, oxidation of substrate is never observed (<5% yield per Mn), thus ruling out the formation of $O{=}Mn^{IV}(TPP)^+$. Furthermore, the lack of epoxidation

(24) (a) Reed, C. A.; Kouba, J. K.; Grimes, C. J.; Cheung, S. K. *J. Am. Chem. Soc.* **1978**, *100*, 3. (b) Hoffman, B. M.; Weschler, C. J.; Basolo, F. *J. Am. Chem. Soc.* **1976**, *98*, 5473.
(25) Hill, C. L. *Activation and Functionalization of Alkanes*, Hill, C. L., Ed.; Wiley: New York, 1989; pp 243–279.

confirms the absence of O=Mn^{IV}(TPP).

Interestingly, oxidation of triphenylphosphine was observed during the photolysis. In the presence of $P(C_6H_5)_3$, 1.01 (3) equiv of $OP(C_6H_5)_3$ per Mn(TPP)(OSO_3H) is formed, and with $[Mn(TPP)]_2(SO_4)$, 0.95 (5) equiv is formed. Due to the fact that metal–oxo species have already been ruled out, this oxidation to $OP(C_6H_5)_3$ most likely does not involve the porphyrin. The ultimate fate of the axial sulfate ligands could not be ascertained. On the basis of charge balance considerations, we may expect $HSO_4^{\bullet}$ or SO_4 diradical to be formed depending on the system in question. The SO_4 diradical is relatively stable toward decomposition to SO_3 and O as well as to SO_2 and O_2.[26] The HSO_4 radical can abstract a hydrogen atom from hydrocarbons,[26] but no oxidative chemistry would result. Detection of these or other possible radical species by spin-trapping was unsuccessful, due to photodecomposition of the traps themselves.

(26) Benson, S. W. *Chem. Rev.* **1978**, *78*, 23.

Conclusions

The new species $[Mn(TPP)]_2(SO_4)$ and Mn(TPP)(OSO_3H) have been synthesized, and their single-crystal X-ray structures show stereochemistry similar to that of the analogous iron complexes. Both manganese compounds are cleanly photoreduced to Mn^{II}(TPP) on irradiation in the region 350–420 nm. In contrast to other manganese oxoanion complexes, no metal–oxo species are formed and no oxidation of hydrocarbons is observed.

Acknowledgment. This work was supported by the National Institutes of Health. We thank Charlotte L. Stern of the University of Illinois X-ray Crystallographic Laboratory for help in performing the structural analyses. We gratefully acknowledge receipt of an NIH Research Career Development Award (K.S.S.) and an NIH Traineeship (R.A.W.).

Supplementary Material Available: Tables of complete atomic coordinates, thermal parameters, and complete bond distances and angles for $[Mn(TPP)]_2(SO_4)$ and Mn(TPP)(OSO_3H) (14 pages). Ordering information is given on any current masthead page.

Contribution from Rhône-Poulenc, Inc., New Brunswick, New Jersey 08901, Lawrence Berkeley Laboratory, Berkeley, California 94720, and Department of Chemistry and Molecular Structure Center, Indiana University, Bloomington, Indiana 47405

Photoreduction of Cerium(IV) in $Ce_2(O^iPr)_8(^iPrOH)_2$. Characterization and Structure of $Ce_4O(O^iPr)_{13}(^iPrOH)$

Kenan Yunlu, Peter S. Gradeff, Norman Edelstein, W. Kot, G. Shalimoff, William E. Streib, Brian A. Vaartstra, and Kenneth G. Caulton*

Received October 4, 1990

Visible irradiation of $Ce_2(O^iPr)_8(^iPrOH)_2$ yields the mixed-valence compound $Ce_4O(O^iPr)_{13}(^iPrOH)$, characterized by ^1H NMR and infrared spectra, elemental analysis, and X-ray diffraction. The structure is described as $Ce_4(\mu_4\text{-}O)(\mu_3\text{-}O^iPr)_2(\mu_2\text{-}O^iPr)_4(O^iPr)_7(^iPrOH)$. The $Ce_4(\mu_4\text{-}O)$ core has a butterfly form, with a crystallographic C_2 axis that passes through the oxide ion and the center of a symmetric hydrogen bond between the coordinated alcohol and one terminal alkoxide. This photoredox reaction cannot be thermally induced and requires that hydrogen be present on the carbon α to the alkoxide oxygen. Magnetic susceptibility and EPR studies show the compound to be paramagnetic. Two temperature ranges of Curie–Weiss behavior are observed with $\mu_{eff} = 2.7\ \mu_B$ from 80 to 300 K. Crystal data (−130 °C): a 21.405 (6) Å, b = 14.077 (3) Å, c = 20.622 (6) Å, and β = 103.97 (1)° with $Z = 4$ in space group $C2/c$.

Introduction

Cerium(IV) has a long tradition as an oxidant in organic chemistry.[1-4] Under acidic aqueous conditions, ethanol is oxidized to acetaldehyde and cyclohexanol to cyclohexanone.[1] In addition to these thermal reactions, photopromotion of certain oxidations has been demonstrated,[5] and Ce(IV) has also been employed in a photolytic splitting of water to give Ce(III), O_2, and H^+.[6] It is reported that the oxidation of methanol to formic acid by Ce(IV) is greatly enhanced by light.[7]

Against this background stands the isolable compound $Ce_2(O^iPr)_8(^iPrOH)_2$,[8,9] which is "stable to about 200 °C under vacuum".[1] We have found that ^{i}PrOH solutions of this compound are photosensitive, and we report here the nature of the product of this reaction.

Experimental Section

All procedures were carried out under an atmosphere of dry dinitrogen or argon or in vacuo. All solvents were appropriately dried and distilled prior to use and stored under dinitrogen.

Infrared spectra were recorded on a Perkin-Elmer 283B spectrometer as Nujol mulls. NMR spectra (^1H, $^{13}C\{^1H\}$) were recorded on Bruker AM-500, WH-90, and AC-200 and JEOL FX 90Q spectrometers and chemical shifts referenced to the protio impurity of the solvent. Elemental analyses were performed at Dornis and Kolbe and Oneida Research Services.

Synthesis of $Ce_4O(O^iPr)_{13}(^iPrOH)$. A solution of $Ce_2(O^iPr)_8(^iPrOH)_2$[8,9] (10 g) in a 2:1 mixture of $MeOC_2H_4OMe/^iPrOH$ (50 mL) was exposed to sunlight for 50 h (not optimized). The color changed to olive green and then orange-brown. Separate experiments in toluene-d_8 showed that, within the first 5 h of photolysis, the sharp ^1H NMR doublet of $Ce_2(O^iPr)_8(^iPrOH)_2$ at 1.28 ppm has converted into a broad singlet at 1.18 ppm, and the final broad singlet spectrum (0.15 ppm) was achieved within 20-h irradiation time. Storage of the reaction solution at −30 °C for 48 h gave orange-brown crystals. Yield: 3.3 g (41%). Anal. Calcd for $C_{42}H_{99}Ce_4O_{15}$: C, 35.91; H, 7.05; Ce, 39.94. Found, C, 36.24; H, 6.81; Ce, 39.82. IR (Nujol mull, cm^{-1}): 3150 (w), 1327 (m), 1152 (sh), 1121 (vs), 982 (vs), 968 (vs), 950 (s), 828 (m), 712 (m), 520 (m), 495 (m), 439 (m). $^{13}C\{^1H\}$ NMR (25 °C, toluene-d_8): 26.85, 71.76. ^1H NMR (500 MHz, toluene-d_8): At 305 K, the dominant species gave a broad resonance centered at δ 0.20, spanning approximately 5 ppm. A sharper resonance at δ 6.00 was also observed, as well as resonances attributed to $Ce_2(O^iPr)_8(HO^iPr)_2$, present as an impurity. As the solution was cooled, the broad resonance collapsed into the baseline (~273 K), and by 193 K, the spectrum displayed a number of sharp singlets. The following major peaks are attributed to the isopropyl groups of $Ce_4O(O^iPr)_{13}(HO^iPr)$: δ −7.96, −6.56, −4.60, −1.36, 0.61, 4.60 (intensity ~1:1:1:1:2:1, C*H*); δ −4.29, −2.10, −0.42, 1.57, 5.91, 6.34, 7.96

* To whom correspondence should be addressed at Indiana University.

(1) Richardson, W. H. In *Oxidation in Organic Chemistry*; Wiberg, K. B., Ed.; Academic Press: New York, 1965; p 24.
(2) Ho, T. *Synthesis* **1973**, 347.
(3) Tomioka, H.; Oshima, K.; Nozaki, H. *Tetrahedron Lett.* **1982**, 539.
(4) Kanemoto, S.; Tomioka, H.; Oshima, K.; Nozaki, H. *Bull. Chem. Soc. Jpn.* **1986**, *59*, 105.
(5) Sheldon, R. A.; Kochi, J. K. *J. Am. Chem. Soc.* **1968**, 90, 6688.
(6) Adamson, A. W.; Fleischauer, P. D. p 252 In *Concepts of Inorganic Photochemistry*; Wiley: New York, 1975; p 252.
(7) Benrath, A.; Ruland, K. *Z. Anorg. Chem.* **1920**, *114*, 267.
(8) Bradley, D. C.; Chatterjee, A. K.; Wardlaw, W. *J. Chem. Soc.* **1956**, 2260; *Ibid.* **1957**, 2600.
(9) Vaartstra, B. A.; Huffman, J. C.; Gradeff, P. S.; Hubert-Pfalzgraf, L. G.; Daran, J.-C.; Parraud, S.; Yunlu, K.; Caulton, K. G. *Inorg. Chem.* **1990**, *29*, 3126.

0020-1669/91/1330-2317$02.50/0